

Theoretical analysis of vertical colloidal deposition

J. J. Diao and J. B. Hutchison

Department of Physics, The George Washington University, Washington, DC 20052

Guanghong Luo

Department of Physics, The George Washington University, Washington, DC 20052

M. E. Reeves^{a)}

Department of Physics, The George Washington University, Washington, DC 20052 and Materials and Sensors Branch, Code 6363, Naval Research Laboratory, Washington, DC 20375

(Received 19 January 2005; accepted 1 March 2005; published online 11 May 2005)

We have modeled the dynamics of a relatively new deposition technique, vertical colloidal deposition (VCD), for preparing nanoparticle thin films. In this process, the substrate is placed vertically in a nanoparticle suspension and is gradually exposed by evaporation or other slow solvent removal. During the film's formation, we observe that the colloidal particles are deposited only at the solid-liquid-gas interface. In contrast with the horizontal geometry, treated elsewhere, where the meniscus is pinned, we observe qualitatively different deposition behaviors. In particular, uniform films rather than rings or lines are produced. Thus, we are led to model a diffusion-driven rather than a convection-driven film growth kinetics, and we are able to predict, consistent with our experimental observations, that the film's areal density is inversely proportional to the descent speed of the suspension surface. Additionally, we find that for submonolayer films, the areal density is proportional to the square of the suspension concentration, converting to a linear dependence once monolayer coverage is attained. © 2005 American Institute of Physics. [DOI: 10.1063/1.1896352]

I. INTRODUCTION

Because of their interesting properties and potential for engineered design, nanoparticles have attracted much focus in materials research. The fundamental questions posed by nanoscale systems are answered while opportunities are created to find unique solutions to technological problems in microelectronics, optoelectronics, and catalysis.¹ Recent results have pointed to the potential contribution of nanoparticles for future technologies. In particular, following the successful control over the size and shape of nanoparticles, there has been considerable interest in exploiting the application of nanoparticles to complex nanoelectronic devices and biochemical sensors.^{2,3} Diverse structures can be constructed using nanoparticles as building blocks, such as ordered spheres and superlattices with the complexity and ordering of the resulting nanostructures dictated by the processing route taken.⁴⁻⁶

There is significant activity devoted to the development of thin-film fabrication methods,⁷ such as layer-by-layer self-assembly,⁸ drying deposition,⁹ and vertical deposition.¹⁰⁻¹⁴ In those approaches, dip coating is certainly a common and simple process for preparing films. More recent work has exploited the air-water-substrate interface as a means to enhance the formation of nanoparticle thin films from low-viscosity suspensions.¹⁵⁻¹⁷ However, there are few models to provide theoretical input for guiding innovations in the latter approach to thin-film fabrication.

This situation exists in spite of significant work on the

dynamics of colloidal motion in evaporating solutions. In particular, studies of nanoparticle deposition and self-assembly onto horizontal substrates and first-principles calculations of the substrate-particle adhesion force have illuminated the role of two-dimensional motion in the meniscus region.¹⁴ Such research has been extended to explain the formation of solute rings arising from evaporating, pinned drops.¹⁸ This, the so-called coffee-ring problem, is explained to stem from the evaporation-driven flow of steadily more concentrated solution to the outer edge of the drop. While the currently accepted models explain the concentration of the solute particles near the outer edge of the drop, they do not address the deposition of material in the meniscus when either the liquid edge is unpinned, or when the solvent reservoir is sufficiently large that the evaporation process does not significantly enrich the colloidal density. The approach reported here addresses this latter class of processes, more akin to vertical deposition, such as the prominent rings formed on the inner surface of a coffee cup.

In our early report,¹⁷ evaporation-driven vertical colloidal deposition (EVCD) is presented as a method to synthesize nanoparticle thin films on substrates positioned vertically, relative to a solution surface. As shown schematically in Fig. 1, when the solution evaporates, more substrate is exposed and coated by the nanoparticle film. The nanoparticles in suspension, within the solid-liquid-gas interface, are deposited on the substrate subject to interfacial forces. Previously, gold nanoparticle thin films have been grown by using EVCD. Typical results of EVCD growth of gold nanoparticle films are pictures in the transmission electron microscopy (TEM) images of Fig. 2, where it is shown that the

^{a)} Author to whom correspondence should be addressed. Electronic mail: reevesme@gwu.edu

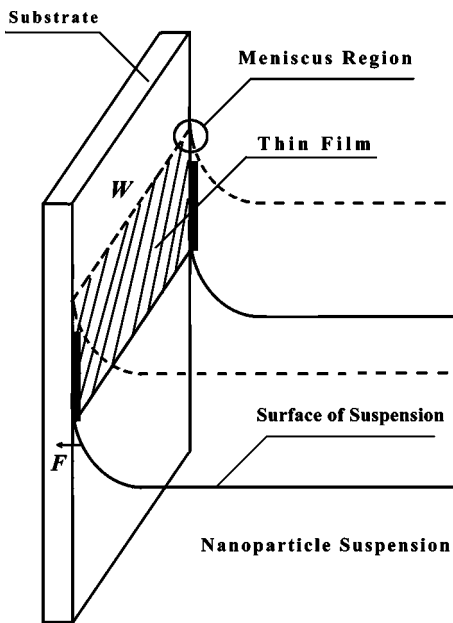


FIG. 1. The schematic of vertical colloidal deposition (VCD) for nanoparticle thin-film synthesis. The substrate is immersed vertically into the nanoparticle suspension, and as the surface of the suspension is lowered, the nanoparticles in meniscus region aggregate on the substrate.

distribution of the gold nanoparticles is homogeneous on a $1\text{--}10\text{-}\mu\text{m}$ scale. Further analysis indicates that nanoparticle films can be made more dense by increasing the concentration of the suspension or by decreasing the descent speed of the suspension surface.¹⁷ Recent work by Im *et al.* has also demonstrated EVCD of latex nanospheres into highly ordered films.¹⁵

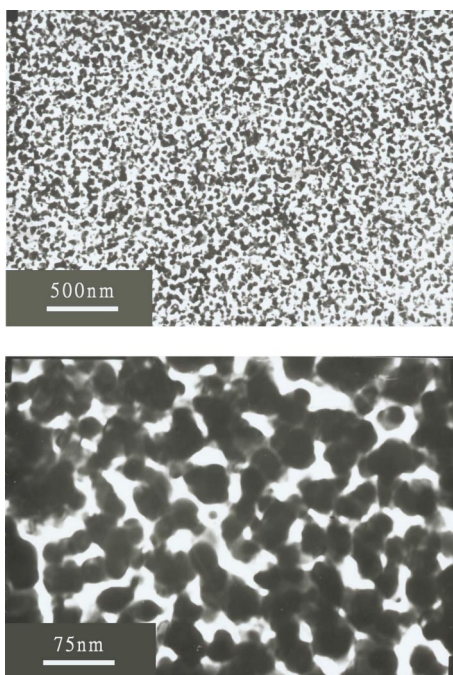


FIG. 2. Transmission electron microscopy (TEM) images of the gold nanoparticle films, made by evaporation-driven vertical colloidal deposition. This and similar micrographs demonstrate that these films are uniform on a $1\text{--}10\text{-}\mu\text{m}$ scale. TEM images of individual nanoparticles indicate that they are spherical and fairly monodispersed.

We note here that evaporation is not a necessary condition, but merely provides a means for slowly dropping the liquid level. In our lab, we have also demonstrated the deposition of nanoparticles when the solution is slowly, but non-evaporatively removed.¹⁹

Motivated by these experiments, we present a theoretical discussion of material transport in the vertical colloidal deposition of nanoparticle thin films. Diffusion theory is used to treat the dynamics of this synthesis process. And in agreement with experiment, our model shows that the areal density of nanoparticles in submonolayer thin films made by EVCD is directly proportional to the square of suspension concentration and inversely proportional to the descent speed of suspension surface. Further, we demonstrate similar behavior for thicker films, except that their areal density is directly proportional to the suspension concentration rather than to its square. The theoretical results obtained in this paper for thicker-than-monolayer nanoparticle films agree well with the experimental trends reported in our earlier results.

II. THEORETICAL ANALYSIS

The dip coating method for preparing thin films is commonly used and models for thin-film formation have been obtained for sol-gel techniques.^{20–22} Recent work has demonstrated the usefulness of dip coating in the low-speed, low-viscosity limit of EVCD,^{15–17,23} but the process has yet to be theoretically described, except for the case in which the substrate is horizontal.²⁴

We have created a quantitative empirical description of the deposition process by simply considering the Brownian motion of nanoparticles in the reduced-dimension, meniscus region of the solution (see Fig 1). This model is useful for optimizing the deposition conditions necessary to obtain desired film morphologies and thicknesses.

Our findings are motivated by our experimental observations of EVCD that the nanoparticle deposition takes place in the thin region of the meniscus rather than in the bulk of the solution. This is crucial. For when the nanoparticle's affinity to the substrate is weak, there is an equal likelihood of adsorption as desorption. There is then no net deposition unless particle motion transverse to the substrate is limited by geometrical constriction. The dynamics of the process is driven by evaporation, which leads the surface of the nanoparticle suspension to drop from the broken line to the solid line of Fig. 1. Then, the nanoparticles in the meniscus aggregate on the substrate and are removed from the suspension, causing a net diffusive flux toward the meniscus region. Hence the deposition speed is limited by rate at which nanoparticles can be replenished by diffusion.

In our discussion of EVCD, two ideal conditions are assumed: the volume change of the suspension is so small that the concentration of the suspension remains constant, and the size of nanoparticles is small enough that the influence of gravity can be ignored.

In our model, the surface of the solution in Fig. 3 descends with speed v . Thus, during a small time Δt the exposed substrate area increases by $\Delta S = Wv\Delta t$, where W is

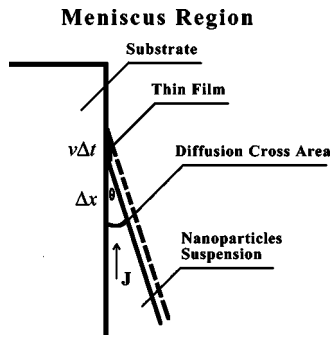


FIG. 3. The process via which nanoparticle thin films are formed by EVCD in meniscus region of the nanoparticle suspension. $v\Delta t$ is distance the suspension surface descends and Δx is the distance that the nanoparticles diffuse in the time interval, Δt . J is the diffusive flux of the nanoparticles, which results in films with densities given by Eq. (5).

the width of substrate immersed in the suspension. The areal density of nanoparticles in the thin film is then by definition

$$N = \frac{\Delta n}{\Delta S} = \frac{\Delta n}{Wv\Delta t}, \quad (1)$$

where Δn is the number of nanoparticles localized on the thin-film area ΔS . Those nanoparticles are suspended in the volume V_{diff} during Δt because of diffusion, and the meniscus is narrow enough that motion within it is constrained to a plane parallel to the substrate. Translational symmetry along the meniscus line reduces the problem to one of quasi-one-dimensional diffusion, the flux of nanoparticles is then governed by Fick's law:²⁵

$$J = -D \frac{\partial C}{\partial x}, \quad (2)$$

where D is the diffusion coefficient, and C is the suspension concentration. The cross-sectional area for diffusion is $ds = W\theta dx$, where θ is the contact angle between the suspension surface and the substrate surface. The number of nanoparticles passing through the cross section is then given as

$$\Delta n = - \int J ds dt = \theta W \int dt \int D \frac{\partial C}{\partial x} dx. \quad (3)$$

In steady state, ΔC is the concentration difference between the bulk suspension and the meniscus. Since not all nanoparticles in the deposition region will aggregate on the substrate, we define ψ as the probability that a given particle will be absorbed upon colliding with the substrate (ψ is treated as a parameter, depending upon forces within the meniscus, see Sec. III). With an amount of $\Delta C = \psi C$ removed from the suspension, Eq. (3) can be written as

$$\Delta n = D\theta W \Delta C \Delta t = D\theta W \psi C \Delta t. \quad (4)$$

By combining this with Eq. (1), we obtain

$$N = \frac{\Delta n}{\Delta S} = \frac{\psi \theta C D}{v}. \quad (5)$$

The coefficient D is given by Einstein's diffusion theory: $D = k_B T / 6\pi\eta r$ (T is the temperature of suspension, η is the viscosity of suspension, k_B is the Boltzmann's constant, and r is the average radius of nanoparticles in suspension). Finally,

combining Einstein's diffusion constant and Eq. (5), we express the areal density of nanoparticles as

$$N = \frac{\psi \theta k_B T C}{6\pi r \eta v}. \quad (6)$$

III. DISCUSSION

A. Factors controlling deposition rate

There are a number of parameters in Eq. (6) which can be determined by simple considerations. For example, according to Einstein's theory of the Brownian motion, the viscosity of the suspension η is given by²⁶

$$\frac{\eta}{\eta_0} = 1 + 2.5 \frac{\bar{V}}{M} C + O(C^2), \quad (7)$$

where η_0 is the viscosity of solvent, and \bar{V} and M are the partial molar volume and molecular weight, respectively. The concentration of the reaction solution is typically in the millimolar range and remains constant through the experiment (since a small volume of liquid evaporates). Thus, in Eq. (7), the concentration-dependent terms are much smaller than 1, allowing us to assume η is a constant, η_0 .¹⁷

The contact angle, θ , between the suspension surface and the substrate is influenced by the solvent, the substrate, and the tilt angle of the substrate relative to the solution.²⁷ This angle is easily measured and even adjusted to control the film's deposition rate. In recent experiments, a steep contact line shape with a small contact angle has demonstrated a lower areal density than a smooth contact line shape with large contact angle,²⁸ as expected from Eq. (6).

The adsorption probability ψ is influenced by the wetting force between the nanoparticle and the substrate. It therefore depends on the substrate, and on the nanoparticle's size, shape, surface properties, and concentration. Some of the conditions for stable attachment of suspended particles to solid surfaces have been previously addressed,²⁹ where, for example, under a barrierless deposition regime, ψ increases in proportion to the bulk suspension concentration. However, once a complete monolayer has been formed, blocking effects become predominate and ψ becomes constant.^{30,31}

Thus, for submonolayer nanoparticle thin films, under equilibrium conditions, the adsorption coefficient, $\psi = KC$, where K is a constant determined by the nanoparticle, solvent, and substrate properties.³⁰ Equation (6) can then be written as

$$N_{\text{submono}} = \alpha_{\text{submono}} \frac{C^2}{v}, \quad (8)$$

where the constant $\alpha_{\text{submono}} = Kk_B T \theta / 6\pi\eta r$. For thicker nanoparticle films, ψ is independent of the suspension concentration,³⁰ and thus, Eq. (6) can be written as

$$N_{\text{thick}} = \alpha_{\text{thick}} \frac{C}{v} + N_{\text{mono}}. \quad (9)$$

$\alpha_{\text{thick}} = \psi k_B T \theta / 6\pi\eta r$ is again constant, as it depends only upon the properties of the nanoparticle, the substrate, and the solvent and upon temperature. N_{mono} is the areal density for

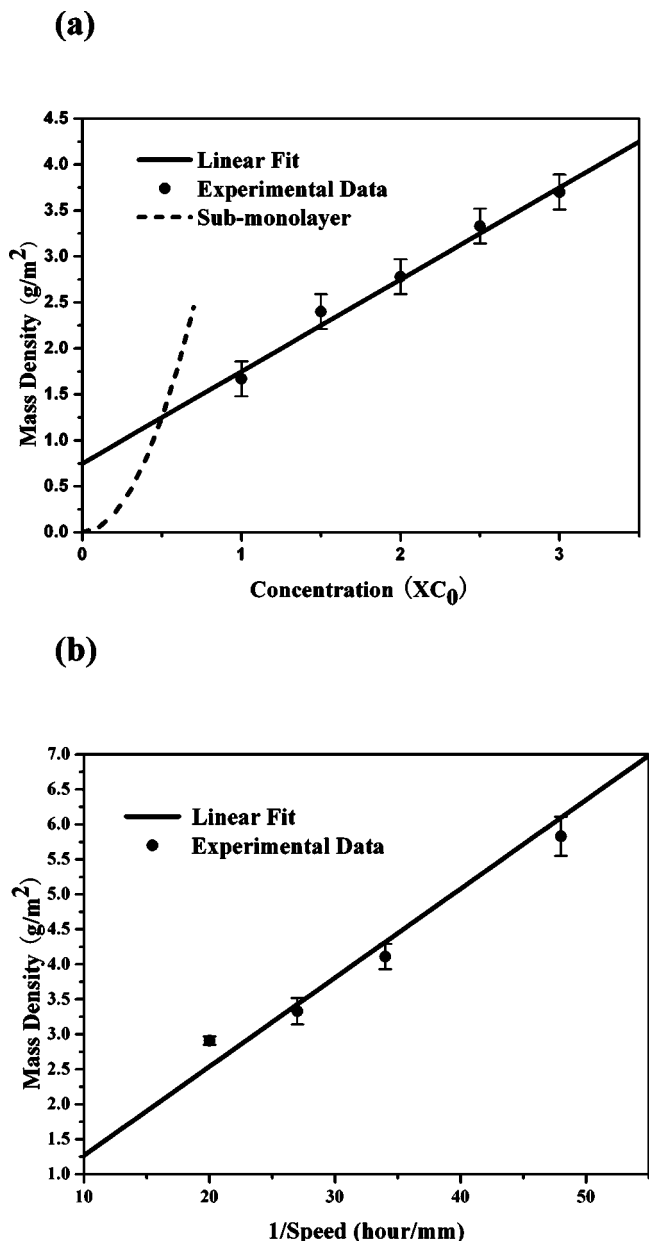


FIG. 4. Experimental results for the deposition of gold nanoparticle films by EVCD. (a) Mass density vs the suspension concentration for a fixed surface descent speed. Film formation initially follows the dotted line, until a complete monolayer is attained. [See Eq. (11)]. From thence, blocking effects lead to a linear dependence with the monolayer offset. (b) The mass density vs the inverse of the surface descent speed of suspension for a fixed concentration. Film densities were determined by weighing films and dividing by their areas. Extremely low deposition rates were obtained by placing the suspension in a humid environment (Ref. 17).

the first monolayer of the nanoparticle thin film.

Equations (8) and (9) demonstrate that the areal density of nanoparticles in a film can be controlled by adjusting the descent speed of the suspension surface and the concentration of suspension. Our previous measurements are consistent with these results, as shown in Fig. 4,¹⁷ that is, with the linear behavior predicted by Eq. (9). In these experiments, the gold nanoparticles in all films are essentially monodispersed as described in Ref. 16, and the areal density is inferred from the mass density. In Fig. 4(a), the dotted line is a representation of the submonolayer film growth curve. The

slopes of the experimental data of Fig. 4, and our knowledge of the nanoparticle concentration, and measurements of the contact angle, allow us to infer the adsorption coefficient for thick films to be greater than 0.6 but less than 0.8.

Finally, the morphology of nanoparticle thin films can be controlled by changing the transition speed of the nanoparticles. In the arrival-limited regime, the nanoparticles have enough time to diffuse at the growth surface to form an ordered structure, unless the transition speed is too large. Then the nanoparticles will form an amorphous film.³²

B. Monolayer nanoparticle thin films

We can demonstrate that for fixed surface descent speed, when the concentration of the suspension is sufficiently low, a submonolayer film will always be deposited. For a known areal density and nanoparticle radius (r), the distance between the nanoparticles for submonolayer films is given by

$$d = \sqrt{\frac{1}{N_{\text{submono}}}} = \sqrt{\frac{6\pi r \eta v}{K \theta k_B T C^2}}. \quad (10)$$

Less than complete coverage is obtained when $d \geq 2r$. Thus, for EVCD, the synthesis condition for submonolayer thin films is

$$\frac{v}{C^2} \geq \frac{2rK\theta k_B T}{3\pi\eta}. \quad (11)$$

Equation (11) shows that for EVCD, a nanoparticle monolayer can be obtained given the proper suspension descent speed and concentration, consistent with our previously reported experimental results.¹⁷

IV. CONCLUSION

A diffusion-based model for evaporation-driven vertical colloidal deposition of nanoparticle thin films is presented in this paper. The trends predicted by these calculations agree with our earlier experiments reported for gold nanoparticle thin films.¹⁷ These results allow us and others to parametrize the deposition conditions for optimal film growth. More experimental data are being obtained for the synthesis of monolayer nanoparticle thin films, guided by the findings reported in this paper.

ACKNOWLEDGMENTS

We thank Professor Z. Adamczyk of Polish Academy of Science for helpful discussion of nanoparticle adsorption, and we thank Dr. Lynn Kurihara, Dr. Dave Pena for helpful comments regarding this manuscript. This work was supported by the Army Research Office (Grant No. DAAD19-01-1-0508).

¹G. Chen, *J. Nanopart. Res.* **2**, 199 (2000).

²A. Bezryadin and C. Dekker, *J. Vac. Sci. Technol. B* **15**, 793 (1997).

³G. A. Ozin and S. M. Yang, *Adv. Funct. Mater.* **11**, 95 (2001).

⁴A. K. Boal, F. Ilhan, J. E. DeRouchey, T. Thurn-Albrecht, T. P. Russell, and V. M. Rotello, *Nature (London)* **404**, 746 (2000).

⁵S. Sun, C. B. Murray, D. Weller, L. Folks, and A. Moser, *Science* **287**, 1989 (2000).

⁶F. Hua, J. Shi, Y. Lvov, and T. Cui, *Nano Lett.* **2**, 1219 (2002).

⁷R. S. Mane and C. D. Lokhande, *Mater. Chem. Phys.* **65**, 1 (2000).

- ⁸G. Decher, *Science* **227**, 1232 (1997).
- ⁹X. M. Lin, H. M. Jaeger, C. M. Sorensen, and K. J. Klabunde, *J. Phys. Chem. B* **105**, 3353 (2001).
- ¹⁰P. Jiang, J. F. Bertone, K. S. Hwang, and V. L. Colvin, *Chem. Mater.* **11**, 2132 (1999).
- ¹¹P. Jiang, J. Cizeron, J. F. Bertone, and V. L. Colvin, *J. Am. Chem. Soc.* **121**, 7957 (1999).
- ¹²Y. H. Ye, F. Lebertone, A. Hache, and V. V. Truong, *Appl. Phys. Lett.* **78**, 52 (2001).
- ¹³L. M. Goldenberg, J. Wagner, J. Stumpe, B. R. Paulke, and E. Gornitz, *Langmuir* **18**, 3319 (2002).
- ¹⁴N. D. Denkov, O. D. Velev, P. A. Kralchevsky, I. B. Ivanov, H. Yoshimura, and K. Nagayama, *Nature (London)* **361**, 26 (1993).
- ¹⁵S. H. Im, Y. T. Lim, D. J. Suh, and O. O. Park, *Adv. Mater. (Weinheim, Ger.)* **14**, 1367 (2002).
- ¹⁶F. Iskandar, M. Abdullah, H. Yoden, and K. Okuyama, *J. Appl. Phys.* **93**, 9237 (2003).
- ¹⁷J. J. Diao, F. S. Qiu, G. D. Chen, and M. E. Reeves, *J. Phys. D* **36**, L25 (2003).
- ¹⁸R. D. Deegan, O. Bakajin, T. F. Dupont, G. Huber, S. R. Nagel, and T. A. Whitten, *Nature (London)* **389**, 827 (1997).
- ¹⁹J. J. Diao, J. B. Hutchison, and M. E. Reeves (unpublished).
- ²⁰C. J. Brinker and G. W. Scherer, *Sol-Gel Science*, 1st ed. (Academic, London, 1990).
- ²¹R. P. Spiers, C. V. Subraman, and W. L. Wilkinson, *Chem. Eng. Sci.* **29**, 389 (1974).
- ²²L. D. Landau and B. G. Levich, *Acta Physicochim. URSS* **17**, 42 (1942).
- ²³G. Bilalbegovic, *Comput. Mater. Sci.* **31**, 181 (2004).
- ²⁴R. D. Deegan, O. Bakajin, T. F. Dupont, G. Huber, S. R. Nagel, and T. A. Whitten, *Phys. Rev. E* **62**, 756 (2000).
- ²⁵H. C. Berg, *Random Walks in Biology*, expanded ed. (Princeton University, Princeton, NJ, 1993).
- ²⁶P. C. Hiemenz and R. Rajagopalan, *Principles of Colloid and Surface Chemistry*, 3rd ed. (Marcel Dekker, New York, NY, 1997).
- ²⁷I. B. Ivanov, A. S. Dimitrov, A. D. Nikolov, N. D. Denkov, and P. A. Kralchevsky, *J. Colloid Interface Sci.* **151**, 446 (1992).
- ²⁸S. H. Im, M. H. Kim, and O. O. Park, *Chem. Mater.* **15**, 1797 (2003).
- ²⁹P. A. Kralchevsky, *Langmuir* **12**, 5951 (1996).
- ³⁰J. Toth, *Adsorption Theory, Modeling, and Analysis*, 1st ed. (Marcel Dekker, New York, NY, 2001).
- ³¹Z. Adamczyk, B. Sihehewek, M. Zembala, and P. Belouschek, *Adv. Colloid Interface Sci.* **48**, 151 (1994).
- ³²C. B. Murray, C. R. Kagan, and M. G. Bawendi, *Annu. Rev. Mater. Sci.* **30**, 545 (2000).